

## Equivalent Time-Domain measurements with noisy signals

by Lionel DUVILLARET

### ABSTRACT

Measurement of repetitive signals using a Digital Sampling Oscilloscope (DSO) is linked to Equivalent Time-Domain (ETD) measurements. Making measurements of noisy signals in ETD leads to a great enhancement of the Signal-to-Noise Ratio (SNR) by making the average of a large number of samples. However, a precise assessment of the signal magnitude needs careful consideration on signal triggering and data analysis.

### INTRODUCTION

Measurement in ETD is necessary when dealing with RF pulsed signals like the ones generated by radars. We consider here some rectangular pulses with a RF carrier at fixed frequency. Such RF pulsed signals can be defined with the following parameters:

- pulse duration  $T$ ,
- pulse rise time  $t_r$ ,
- pulse fall time  $t_f$ ,
- signal carrier frequency  $f_s$ ,
- signal Root Mean Square (RMS) [1] value  $S_{RMS}$ ,
- noise RMS value  $N_{RMS}$ ,
- sampling interval  $\delta t$ ,
- signal phase at origin ( $t = 0$ )  $\varphi_s$ ,
- pulse repetition frequency  $PRF$ .

They are well described by the analytical formula (1).

$$V(t) = (S_{RMS}/\sqrt{8}) \cos(2\pi f_s t + \varphi_s) \text{erfc}(2(t-T)/t_f) (2 - \text{erfc}(2t/t_r)) * \mathbb{I}_{1/PRF}(t) + \sqrt{2} N_{RMS} \chi(t) \quad (1)$$

where  $*$  denotes the convolution product,  $\mathbb{I}$  is the Dirac comb function and  $\chi(t)$  is a random variable with a standard normal distribution [2].

From here, we consider:

- 1- $\mu$ s RF pulsed signals with 5-ns rise & fall times,
- a 400-MHz carrier frequency with a zero phase value  $\varphi_s$ ,
- a 50-ps sampling interval (20 GSa/s),
- a 1-kHz pulse repetition frequency  $PRF$ ,
- a 100-mV noise RMS value  $N_{RMS}$ .

All results presented hereafter have been carried out with Monte-Carlo simulations.

### TRIGGER AND JITTER ISSUE

The first important issue concerns the signal triggering when dealing with noisy signals. Fig. 1 represents a single shot record of a 10-mV signal carrier RMS value.

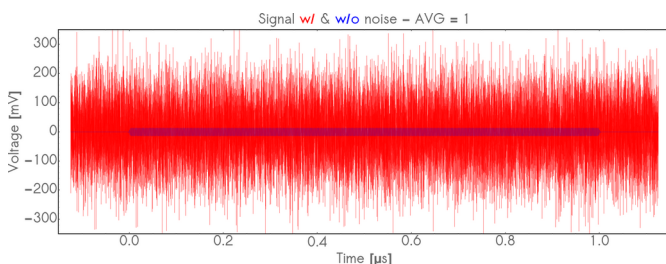


Fig. 1 - Single shot record of signal with and without noise

As seen on Fig. 1, the zone over which the signal carrier is present is impossible to discriminate. With such ultra low single-shot SNR (0.1), the record of the signal is only possible if the DSO is triggered by the source of the signal carrier itself and not by the noisy signal. This is a key point for measuring noisy signals (see Fig. 2).

### EQUIVALENT TIME-DOMAIN ISSUE: Required setup

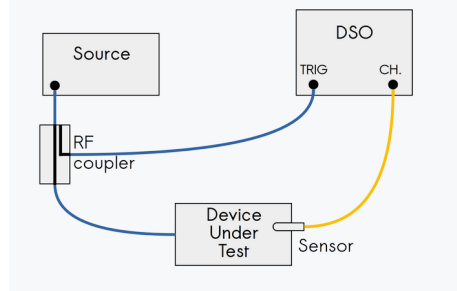


Fig. 2 - Required setup for accurate measurements with noisy signals

Making an average of  $N = 100$  samples will reduce the noise RMS value by a factor  $\sqrt{N} = 10$ . For the signal carrier, its averaged value depends on the DSO jitter [3]  $J_{DSO}$  (considered as Gaussian) on the one hand, and on the stability of the source of the signal carrier on the other hand. This latter one is here considered as perfect.

Fig. 3 to 6 represent records for an average of 100 samples of a 10-mV signal carrier RMS value with different DSO jitter values:

- $J_{DSO} = 1$  ns ( $1 / 2.5 f_s$ ) for Fig. 3
- $J_{DSO} = 500$  ps ( $1 / 5 f_s$ ) for Fig. 4
- $J_{DSO} = 250$  ps ( $1 / 10 f_s$ ) for Fig. 5
- $J_{DSO} = 125$  ps ( $1 / 20 f_s$ ) for Fig. 6

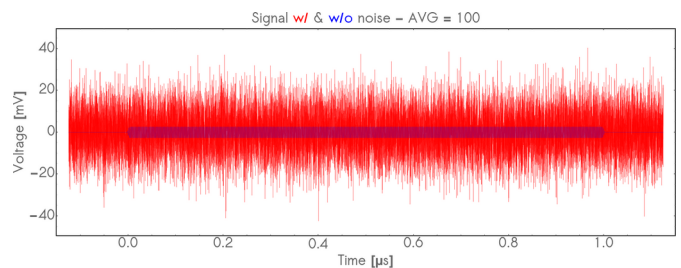


Fig. 3 - Record for  $N = 100$  Sa with a RMS jitter of 1 ns

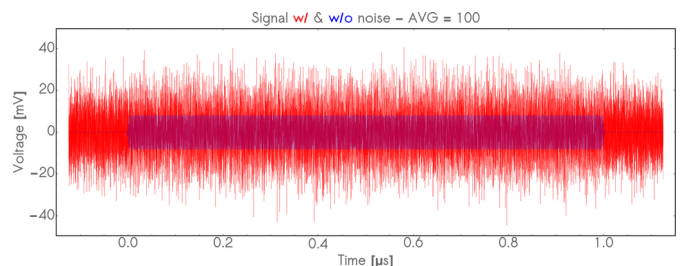


Fig. 4 - Record for  $N = 100$  Sa with a RMS jitter of 500 ps

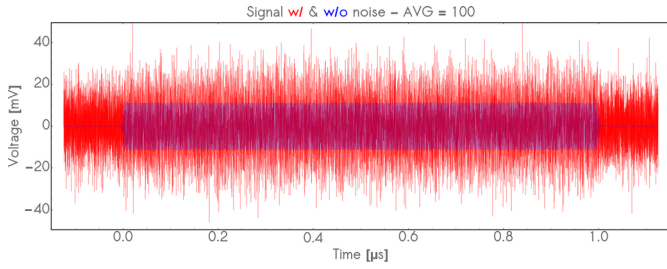


Fig. 5 - Record for  $N = 100$  Sa with a RMS jitter of 250 ps

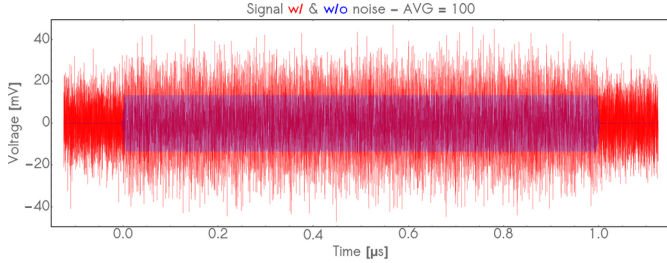


Fig. 6 - Record for  $N = 100$  Sa with a RMS jitter of 125 ps

The smaller the DSO jitter compared to  $1/f_s$ , the higher the SNR gain. Fig. 7 shows SNR evolution versus  $N$  and  $J_{DSO}$ .

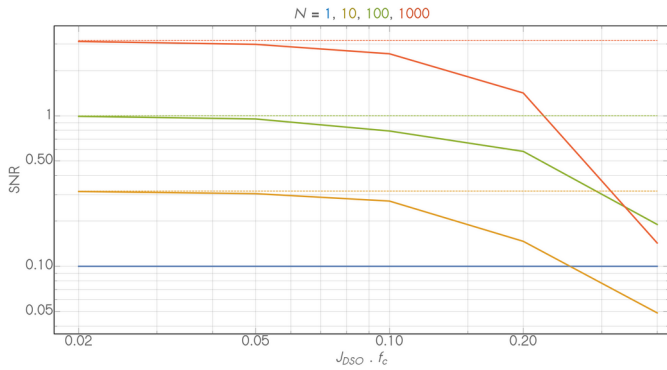


Fig. 7 - SNR as function of  $N$  and  $J_{DSO} \cdot f_s$  product

As seen, if the DSO presents an important jitter, it could be even worse to take the average of a large number of samples. Taking the average does not induce any significant deviation from theory (dashed horizontal lines) as soon as the product  $J_{DSO} \cdot f_s$  is lower than 0.02. For a carrier frequency of 5 GHz, the RMS DSO jitter must be lower than 4 ps. With ultra high-grade oscilloscope presenting sub-100 fs jitter, measurements can be carried out up to 70 GHz.

Fig. 8 shows the record obtained for an average of  $N = 1000$  samples.

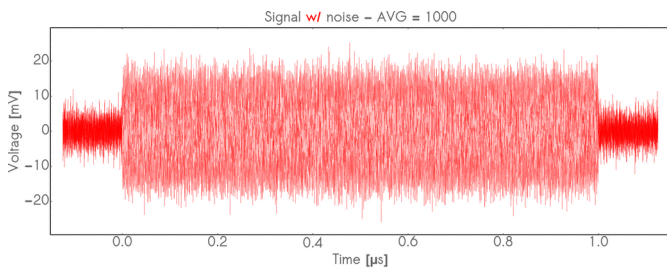


Fig. 8 - Record for  $N = 1000$  Sa with a RMS jitter of 50 ps

From Fig. 1 to Fig. 8, the only parameter that has changed is the number of samples on which the signal has been averaged. On that record, the signal appears very clearly even if the SNR  $\sim 3$  is still low.

#### ASSESSMENT OF SIGNAL MAGNITUDE

A rather precise assessment of the signal carrier RMS value can be obtained from the RMS values given by the DSO for the zones without ( $t < 0$  or  $t > 1$   $\mu$ s) and with signal (for  $0 < t < 1$   $\mu$ s). Tab. 1 sums up the calculated values. Let us remind that signal and noise are generally uncorrelated, leading to the fact that the signal and noise powers are added together. This is summarized in Eq. (2).

$$V_{RMS}^2 = S_{RMS}^2 + N_{RMS}^2 \quad (2)$$

Tab. 1 -4<sup>th</sup> column- gives the signal carrier calculated RMS value  $S_{RMS}$  from the data represented in the different figures above. Let us remind that the true signal carrier RMS value is precisely 10 mV. As seen, the true carrier RMS value  $\langle S_{RMS} \rangle$  -5<sup>th</sup> column-, obtained by an average on a large number of samples, differs from the true signal carrier RMS value because of the strong DSO jitter. Both values are equal only for the case represented in Fig. 1 as it corresponds to a single shot record. In the case represented in Fig. 8, the signal carrier calculated RMS value is only 1% lower than the true signal carrier RMS value (10 mV) even if the SNR is only  $\sim 3$ .

With a RMS DSO jitter ten times smaller (5 ps -  $J_{DSO} \cdot f_s = 0.002$ ), this difference decreases to an insignificant value of 0.03%.

Fig.	$N_{RMS}$ [mV] ( $t < 0$ or $t > 1$ $\mu$ s)	$V_{RMS}$ [mV] ( $0 < t < 1$ $\mu$ s)	$\sqrt{(V_{RMS}^2 - N_{RMS}^2)}$ [mV]	True $\langle S_{RMS} \rangle$ value	Difference
1	99.4	99.8	8.93	10.00	-10.7%
2	10.01	10.17	1.80	1.90	-5.3%
3	9.98	11.52	5.75	5.79	-0.7%
4	10.03	12.83	8.00	7.95	-0.6%
5	10.02	13.81	9.50	9.55	-0.5%
7	3.18	10.40	9.90	9.92	-0.2%

Tab. 1 - Signal carrier calculated RMS value  $S_{RMS}$  for the different configurations represented in Fig. 1 to 5 and 7

Whereas peak-to-peak voltage  $V_{pp}$  is directly linked to RMS voltage  $V_{RMS}$  for noise-free RF pulsed signals ( $V_{pp} = 2\sqrt{2} V_{RMS}$ ), this is no more the case for noisy signals. For the example of the record of Fig. 8, we have  $V_{RMS} = 10.50$  mV and  $V_{pp} = 51.07$  mV which is far from its expected value of 29.70 mV.

#### OFFSET ISSUE

For different reasons, an offset could occur on the record like the one represented in Fig. 9: voltage offset is set here to 5 mV.

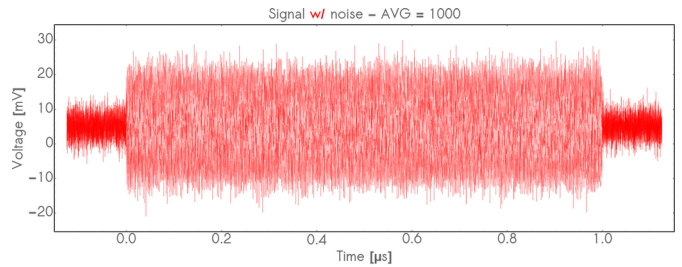


Fig. 9 - Record for  $N = 1000$  Sa with a RMS jitter of 50 ps and a voltage offset of 5 mV

The only difference between Monte-Carlo simulations of Fig. 8 and 9 concerns the voltage offset. For records of Fig. 8 and 9, we get:

- $V_{RMS} = 11.62$  mV and 10.50 mV, respectively,
- $N_{RMS} = 5.92$  mV and 3.17 mV, respectively.

Indeed, when we are dealing with signals with non-zero average, it is no more the RMS values that should be taken into account but the standard deviations  $\sigma$ . However both values are related each other through Eq. (3).

$$X_{RMS}^2 = \sigma^2 + \mu^2 \quad (3)$$

where  $\mu_X$  represents the average of variable  $X$ . Having  $\mu_V = \mu_N = 5$  mV, we can easily calculate  $\sigma_V$  and  $\sigma_N$  from  $V_{RMS}$  and  $N_{RMS}$ . We obtain:

- $\sigma_V = \sqrt{(11.62^2 - 5^2)} = 10.49$  mV,
- $\sigma_N = \sqrt{(5.92^2 - 5^2)} = 3.17$  mV.

For the more general case, the expression of the signal carrier RMS value  $S_{RMS}$  is given by Eq. (4).

$$S_{RMS} = \sqrt{\{(V_{RMS}^2 - \mu_V^2) - (N_{RMS}^2 - \mu_N^2)\}} \quad (4)$$

where:

- $V_{RMS}$  is the RMS value given by the DSO for the zone with the signal ( $0 < t < 1$   $\mu$ s),

- $\mu_V$  is the average value given by the DSO for the zone with the signal ( $0 < t < 1 \mu s$ ),
- $N_{RMS}$  is the RMS value given by the DSO for the zone without the signal ( $t < 0$  or  $t > 1 \mu s$ ),
- $\mu_N$  is the average value given by the DSO for the zone without the signal ( $t < 0$  or  $t > 1 \mu s$ ).

### PRACTICAL APPLICATION

For that practical application the experimental setup, shown in Fig. 10, is composed of:

- a synthesizer Agilent 83640 B,
- a  $50\Omega$  impedance DSO MSO-X 3104 A (1-GHz bandwidth),
- an E-field probe Kapteos eoProbe EL5-air (10-GHz bandwidth),
- a probe-related optoelectronic converter Kapteos eoSense MF-1S (1-GHz bandwidth),
- an ATEM cell Kapteos eoCal HF-6 (6-GHz bandwidth).

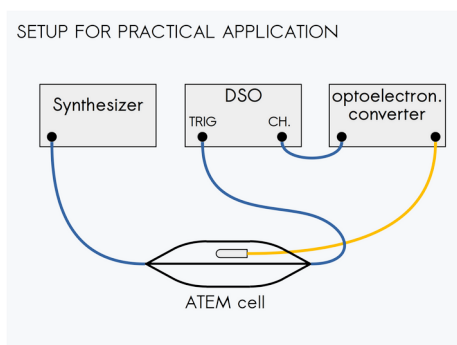


Fig. 10 - Experimental setup

Both synthesizer and DSO have been configured as follows:

- 2- $\mu s$  RF pulsed signals with fast rise & fall times,
- a 50-MHz carrier frequency with 17-dBm RF power,
- a 2.5-ns sampling interval (400 MSa/s),
- a 166.67-kHz pulse repetition frequency  $PRF$ .

For these parameters, the magnitude of the E-field in the ATEM cell is  $93 V_{rms}/m$ , the E field direction being vertical. The sensitivity axis of the E-field probe making an angle of  $60^\circ$  with respect to the vertical, the effective E field seen by the probe EL5-air is finally only  $47 V_{rms}/m$ .

Fig. 11 to 14 show the records obtained for an average of  $N = 2$ , 64, 2048 and 65536 samples, respectively.

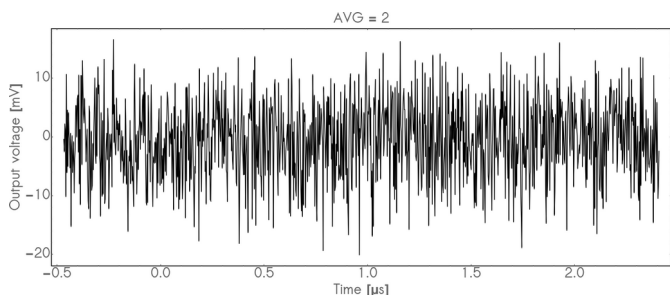


Fig. 11 - Record for an effective E-field strength of  $47 V_{rms}/m$  and  $N = 2 Sa$

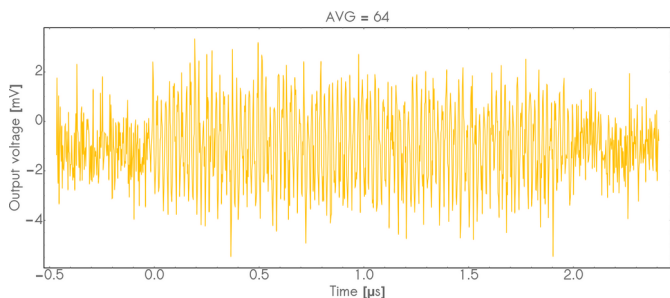


Fig. 12 - Record for an effective E-field strength of  $47 V_{rms}/m$  and  $N = 64 Sa$

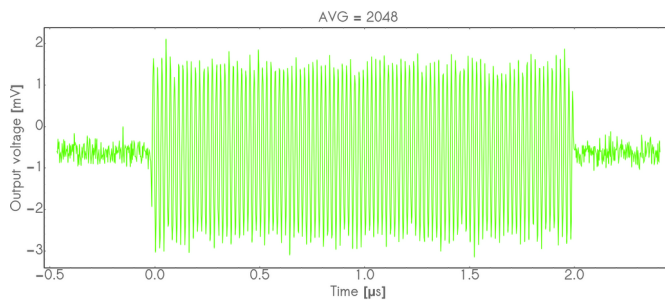


Fig. 13 - Record for an effective E-field strength of  $47 V_{rms}/m$  and  $N = 2048 Sa$

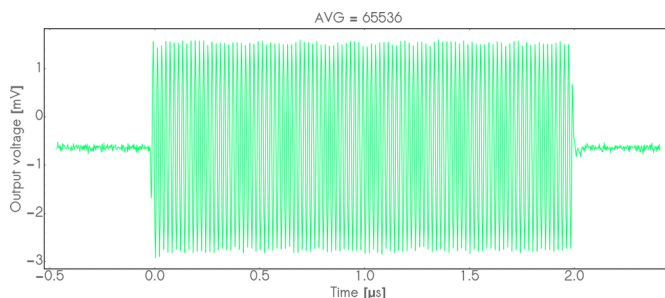


Fig. 14 - Record for an effective E-field strength of  $47 V_{rms}/m$  and  $N = 65536 Sa$

A high SNR is obtained with  $N = 65536$  samples (Fig. 14) while the signal is not visible with  $N = 2$  samples (Fig. 11). For  $N = 64$  samples (Fig. 12), we can distinguish the presence of the signal even if it seems unusable for an accurate assessment of its magnitude. Fig 15 exhibits how the SNR increases with  $N$ .

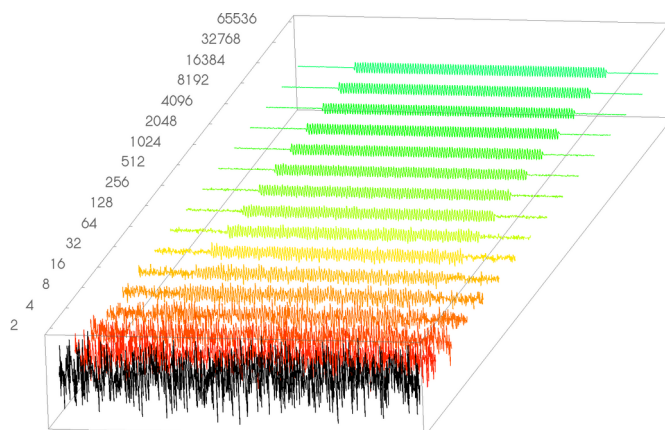


Fig. 15 - Signal evolution with number of samples  $N$

As seen on Fig. 12 to 14, the offset is presently an issue. Therefore, let us now apply formula (4) for all records presented in Fig. 15. For that purpose we have used the automatic measurements carried out by the DSO (see Tab. 2).

$N$	$V_{RMS}$ [mV]	$\mu_V$ [mV]	$N_{RMS}$ [mV]	$\mu_N$ [mV]	$S_{RMS}$ [mV]
2	7.4	-1	7.25	-1	1.482 (-3.4%)
4	5.1	-0.9	4.8	-0.9	1.723 (+12.3%)
8	3.7	-0.9	3.3	-0.9	1.673 (+9.0%)
16	2.72	-0.95	2.32	-0.9	1.387 (-9.6%)
32	2.32	-0.92	1.76	-0.92	1.512 (-1.5%)
64	2.03	-0.9	1.4	-0.9	1.470 (-4.2%)
128	1.86	-0.81	1.1	-0.82	1.505 (-1.9%)
256	1.77	-0.78	0.95	-0.79	1.499 (-2.3%)
512	1.72	-0.78	0.85	-0.76	1.485 (-3.2%)
1024	1.65	-0.64	0.71	-0.65	1.494 (-2.7%)
2048	1.645	-0.632	0.665	-0.64	1.508 (-1.7%)
4096	1.64	-0.621	0.665	-0.65	1.511 (-1.5%)
8192	1.64	-0.647	0.655	-0.655	1.507 (-1.8%)
16384	1.64	-0.64	0.65	-0.64	1.506 (-1.9%)
32768	1.66	-0.649	0.64	-0.639	1.527 (+0.5%)
65536	1.67	-0.656	0.66	-0.657	1.534 (Ref. value)

Tab. 2 - Calculation table of  $S_{RMS}$  for records represented in Fig. 15

As seen on Tab. 2, the signal carrier RMS value  $S_{RMS}$  is accurately assessed ( $\pm 2\%$ ) down to  $N = 2048$  (see Fig. 13). From  $N = 1024$  down to  $N = 64$  (see Fig. 12), we keep a rather good assessment ( $\pm 5\%$ ) of the signal carrier RMS value.

The link between the automatic measurements carried out by the DSO and the terms of Eq. (4) are summarized in Tab. 3.

Variable of Eq. (4)	DSO automatic measurement	Part of signal to be displayed on DSO before automatic measurements
$V_{RMS}$	DC-RMS-FS	Record part corresponding to the presence of the signal carrier, i.e. for example in a 1- $\mu$ s time window for interval $t[\mu s] \in [0.5, 1.5]$ (see Fig. 14)
$\mu_V$	AVG-FS	
$\sqrt{(V_{RMS}^2 - \mu_V^2)}$	AC-RMS-FS	Record part corresponding to the absence of signal, i.e. for example in a 1- $\mu$ s time window for interval $t[\mu s] \in [2.5, 3.5]$ (see Fig. 14)
$N_{RMS}$	DC-RMS-FS	
$\mu_N$	AVG-FS	
$\sqrt{(N_{RMS}^2 - \mu_N^2)}$	AC-RMS-FS	

Tab. 3 - Correspondence table between Eq. (4) terms and automatic measurements carried out by the DSO

When dealing with noisy signals, it is always very interesting to plot both terms  $\sqrt{(V_{RMS}^2 - \mu_V^2)}$  and  $\sqrt{(N_{RMS}^2 - \mu_N^2)}$  versus  $N$  (see Fig. 16) as it reveals very efficiently possible trigger/jitter issue and also if the noise is or is not a Gaussian noise fully uncorrelated with the signal. These two terms  $\sqrt{(V_{RMS}^2 - \mu_V^2)}$  and  $\sqrt{(N_{RMS}^2 - \mu_N^2)}$  are directly obtained from DSO automatic measurements (see Tab. 3).

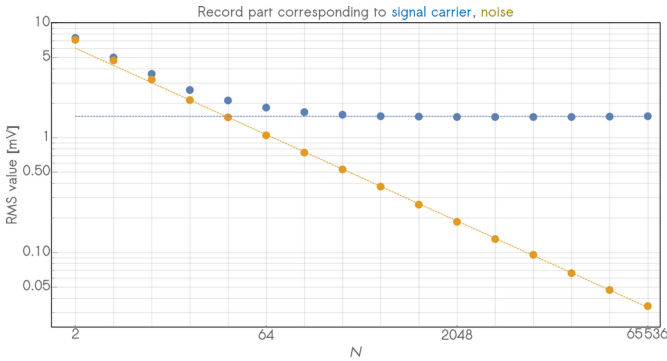


Fig. 16 - Plot of  $\sqrt{(V_{RMS}^2 - \mu_V^2)}$  and  $\sqrt{(N_{RMS}^2 - \mu_N^2)}$  versus  $N$

As seen in Fig. 16, term  $\sqrt{(V_{RMS}^2 - \mu_V^2)}$  converges towards the true signal carrier RMS value (dotted blue line) whereas term  $\sqrt{(N_{RMS}^2 - \mu_N^2)}$  is decreasing as  $1/\sqrt{N}$  (dotted brown line) as expected for a Gaussian noise fully uncorrelated with the signal. The SNR is given by the ratio between these two terms: it is  $\sim 2$  for  $N = 64$ . It is remarkable that, even with such low SNR (see Fig. 12), Eq. (4) gives the signal carrier RMS value with an error lower than 5%!

As term  $\sqrt{(V_{RMS}^2 - \mu_V^2)}$  converges towards a constant, this means that neither trigger nor jitter constitutes an issue. Indeed, as soon as trigger or jitter is an issue, the term  $\sqrt{(V_{RMS}^2 - \mu_V^2)}$  does not converge anymore towards a constant but decreases with  $N$ .

### TO GO FURTHER

To go further, it is necessary to move from the time-domain to the frequency-domain using a Fast Fourier Transform (FFT) [4] or to implement an analytical fitting of the recorded data using Eq. (1) in case of rectangular pulses with a RF carrier at fixed frequency. This latter solution is by far the one leading to the more accurate assessment of the signal carrier RMS value and also to other important pulse parameters like  $T$ ,  $t_r$ ,  $t_f$ ,  $f_c$  and  $\phi$ .

Fig. 17 to 20 show both records and fits given by Eq. (1) for an average of  $N = 2, 64, 2048$  and  $65536$  samples, respectively.

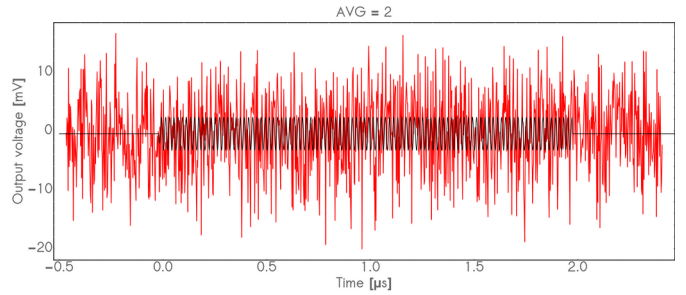


Fig. 17 - Record for an effective E-field strength of  $47 V_{rms}/m$  and  $N = 2 Sa$  with its best fit given by Eq. (1)

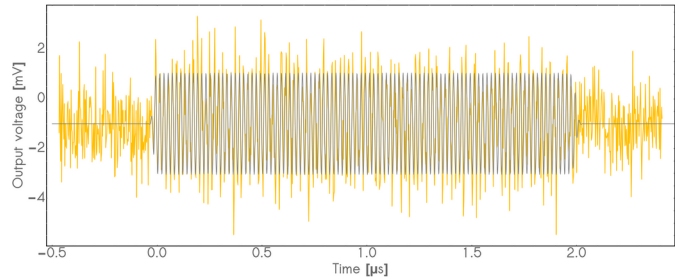


Fig. 18 - Record for an effective E-field strength of  $47 V_{rms}/m$  and  $N = 64 Sa$  with its best fit given by Eq. (1)

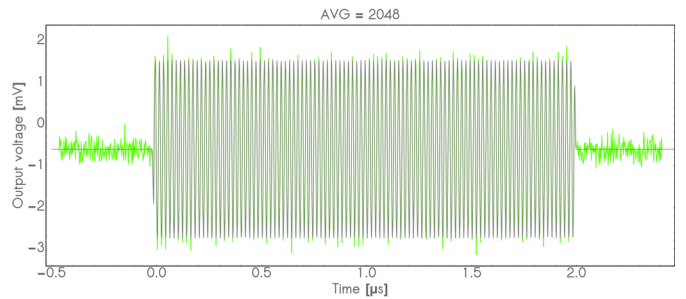


Fig. 19 - Record for an effective E-field strength of  $47 V_{rms}/m$  and  $N = 2048 Sa$  with its best fit given by Eq. (1)

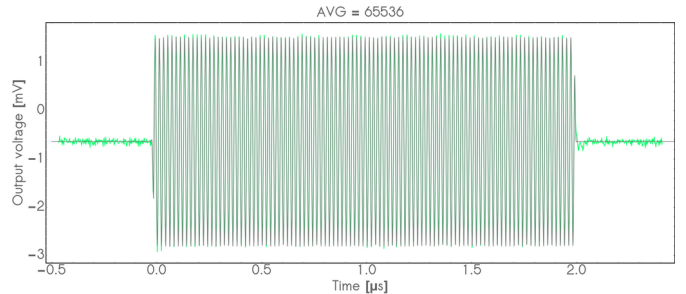


Fig. 20 - Record for an effective E-field strength of  $47 V_{rms}/m$  and  $N = 65536 Sa$  with its best fit given by Eq. (1)

The fitting parameters of Fig. 17 to 20 are given in Table 4 with their calculated uncertainties.

Fitting parameter	$N = 65\ 536$ (cf. Fig. 20)	$N = 2\ 048$ (cf. Fig. 19)	$N = 64$ (cf. Fig. 18)	$N = 2$ (cf. Fig. 17)
Carrier frequency [MHz]	50 $\pm 0.0003$	50 $\pm 0.001$	50 $\pm 0.007$	50 $\pm 0.032$
Signal carrier RMS value [mV]	1.524 $\pm 0.002$	1.502 $\pm 0.006$	1.427 $\pm 0.034$	1.96 $\pm 0.23$
Signal phase at $t = 0$ [°]	187.5	185	154	181
Rise time [ns]	$11 \pm 1$	$8 \pm 3$	$21 \pm 22$	$11 \pm 100$
Fall time [ns]	$8 \pm 0.8$	$6 \pm 2$	$32 \pm 27$	$0 \pm 120$
Pulse duration [ $\mu$ s]	$2.0096 \pm 0.0002$	$2.0099 \pm 0.0006$	$2.014 \pm 0.009$	$1.992 \pm NA$
Offset [mV]	$-0.638 \pm 0.002$	$-0.605 \pm 0.005$	$-0.997 \pm 0.028$	$-0.480 \pm 0.190$
Pulse beginning [ns]	$-16.7 \pm 0.2$	$-16.8 \pm 0.5$	$-18.6 \pm 5.4$	$-16.9 \pm 1.8$

Tab. 4 - Fitting parameters of Fig. 17 to 20

Both carrier frequency, pulse duration & beginning are determined with a very good to excellent accuracy, even for  $N = 2$ . Signal carrier RMS value is here determined with the order of magnitude of its accuracy, contrary to its assessment from DSO automatic measurements. Such analysis gives also a much better insight into the signal carrier. Moreover, the validity of the fit can be very easily checked visually in Fig. 18 to 20.

#### SUMMARY

When dealing with noisy RF pulsed signals in ETD, it should be checked that the RMS DSO jitter is lower than  $0.02 / f_s$  where  $f_s$  is the signal carrier frequency. The measurement setup has to be compliant with the one represented in Fig. 2. Then, for both zones with and without signal, the following parameters calculated by the DSO have to be recorded:

- the RMS values  $V_{RMS}$  and  $N_{RMS}$ , respectively,
- the average values  $\mu_V$  and  $\mu_N$ , respectively.

Finally, using Eq. (4), an accurate value of the signal carrier RMS value  $S_{RMS}$  can be assessed even with very noisy signals (see Fig. 12). Moreover, using the fitting Eq. (1), much more precise and complementary information can be assessed (see Fig. 18).

#### REFERENCES

- [1] [https://en.wikipedia.org/wiki/Root\\_mean\\_square](https://en.wikipedia.org/wiki/Root_mean_square)
- [2] [https://en.wikipedia.org/wiki/Normal\\_distribution](https://en.wikipedia.org/wiki/Normal_distribution)
- [3] <https://en.wikipedia.org/wiki/Jitter>
- [4] [https://en.wikipedia.org/wiki/Fast\\_Fourier\\_transform](https://en.wikipedia.org/wiki/Fast_Fourier_transform)